

Ground state structure and interactions between dimeric 2D Wigner crystals

V. LOBASKIN and R. R. NETZ

Physics Department, Technische Universität München, James-Frank-Str., D-85747 Garching, Germany

PACS 82.70.-y – Disperse systems; complex fluids

PACS 64.70.Kb – Solid-solid transitions

PACS 68.47.Pe – Langmuir-Blodgett films on solids; polymers on surfaces; biological molecules on surfaces

Abstract. - We study the ground state ordering and interactions between two two-dimensional Wigner crystals on neutralizing charged plates by means of computer simulation. We consider crystals formed by (i) point-like charges and (ii) charged dimers, which mimic the screening of charged surfaces by elongated multivalent ions such as aspherical globular proteins, charged dendrimers or short stiff polyelectrolytes. Both systems, with point-like and dimeric ions, display five distinct crystalline phases on increasing the interlayer distance. In addition to alteration of translational ordering within the bilayer, the phase transitions in the dimeric system are characterized by alteration of orientational ordering of the ions.

The interaction between electric double layers attracted much attention in the past twenty years in particular due to the rediscovered role of ionic correlations. It has been known for long time that two similarly and strongly charged plates can attract each other in the presence of multivalent counterions. This has been seen in Monte Carlo simulations [1–3], observed experimentally with the surface force apparatus [4], deduced from the scattering experiments on laponite dispersions [5], phase diagrams of charged lamellar systems [6, 7], clay platelets, etc. (see [8–10] for a review).

As the attraction appears on increasing counterion correlations, the phenomenon can be conveniently characterized by an electrostatic coupling parameter $\Xi = 2q^3 l_B^2 \sigma_s$, which depends on the Bjerrum length l_B , the counterion valency q , and the surface charge density σ_s . Several successful descriptions of the attraction have been built for the strong coupling limit $\Xi \rightarrow \infty$, where the correlations are so strong that the ions form a Wigner crystal (WC) [11] or at least a strongly correlated liquid (SCL) at the charged colloid surface [12, 13].

Although the phase diagram of a bilayer Wigner crystal has been known for some time both at the ground state and at finite temperature [14–18], the interaction between the crystalline double layers as a function of their separation has not been discussed in detail. The mono- and bilayer Wigner crystal structures have been addressed in literature in relation to electrons above the surface of liquid helium, two-dimensional semiconductor heterostructures, Mott insulators, dusty plasmas, laser-beam-cooled trapped-ion plasmas, or dislocation-mediated melting transitions [19, 20]. In contrast, in the soft-matter and biological literature the crystal structure is typically

regarded as an auxiliary question for evaluating the interactions between the surfaces that host these Wigner crystals [21–23]. Typically, only the staggered hexagonal crystal, which wins at large distances, is considered. A few recent publications discuss interaction effects such as plasmon oscillations using perturbation schemes with respect to the ground state of the double layers at large distances (the staggered hexagonal phase) [21, 22].

A characteristic feature that differentiates Wigner crystals in soft matter systems from the low-temperature electronic ones stems from the nature of the ions: The ions have to be multivalent to be well ordered in aqueous dispersions. The high ion valency also implies that the Coulomb contribution dominates the free energy and in-layer thermal fluctuations are negligible. A situation close to the low-temperature behaviour can be obtained, for example, when polyelectrolyte molecules, globular proteins or charged dendrimers play the role of counterions [24–26]. In the general case, such ions are neither point-like nor spherical and their shape might influence the interaction between the bilayers. For example, in the limit of very long ions (DNA chains between lipid bilayers) their anisotropy leads to orientational ordering and formation of two-dimensional smectic phases [27, 28]. In this work, we present an accurate numerical solution of the ground state problem both for point-like (spherical) and small but elongated (non-spherical) counterions. We first address the interaction between the bilayers with point-like ions and then use it as a reference system to study the effect of ion size and charge distribution on the bilayer interaction.

We envision a situation where the interaction energy for two flat parallel Wigner crystals on a neutralizing background is measured as a function of the interlayer distance.

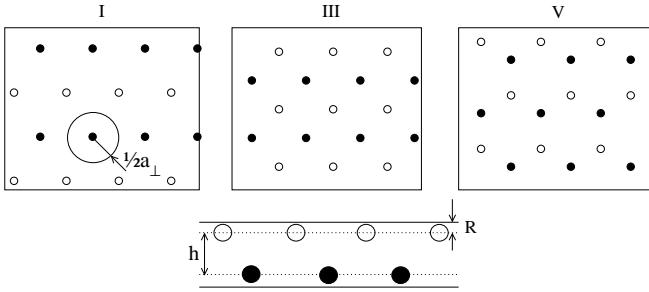


Fig. 1: Top and side view of three 2D configurations of counterions on two parallel charged plates. The open and filled symbols designate the ions located on the opposite surfaces. Set I corresponds to a single hexagonal lattice, Set III to a superposition of two square lattices, and Set V corresponds to two staggered hexagonal lattices (the notation is explained in the text).

For point-like ions the scenario includes two obvious limiting cases: at large separations, the crystals do not feel any discreteness of each other so that each of them has a 2D plane-filling hexagonal symmetry. At the smallest separation between them, where both of them lie in the same plane, a single hexagonal crystal is formed. At a finer resolution, the transition between these two phases gives rise to the following sequence of structures on increasing the interlayer distance: a monolayer hexagonal lattice (I), a staggered rectangular lattice (II), a staggered square lattice (III), a staggered rhombic lattice (IV), and a staggered hexagonal lattice (V) [14]. Here, we evaluate the ground state interaction by minimizing the energy at each gap width and in addition, consider three particular phases in more detail. Namely, we consider three setups, for which the positions of ions on one plane fall in the geometrical centres of the primitive cells of the identical lattice on the other plane: the hexagonal monolayer structure (I); staggered square lattice (III); and staggered hexagonal lattice (V). These three configurations are shown in Fig. 1. They represent the three rigid lattices on the bilayer phase diagram, meaning that their structure does not change within their region of stability. The intermediate structures (II and IV) are "soft", so that the aspect ratio of their primary cell is varying with the interlayer distance [14]. Finally, to study the effect of the ion shape we replace each ion by a dimer consisting of two identical charges connected by a stiff spring. The dimer is allowed to rotate and translate in plane and two different spring lengths are studied.

The energy of a Wigner crystal on a neutralizing charged plane can be written as

$$U_1 = \sum_{j=1}^{N-1} \sum_{k=j+1}^N \frac{q^2}{\epsilon |\mathbf{r}_j - \mathbf{r}_k|} + \sum_{j=1}^N \frac{2\pi q_j \sigma_s R}{\epsilon} \quad (1)$$

where σ_s is the surface charge density of the plate, q the counterion charge, N the number of counterions, ϵ the dielectric permittivity of the medium, and R the ion-plate contact distance, or the ion radius for hard sphere ions.

The characteristic lengthscale of the Wigner crystal on a neutralizing background is the mean lateral distance between the ions a_\perp , which is defined by $\pi (a_\perp/2)^2 = q/\sigma_s$. The energies can be conveniently expressed in terms of the average ion-ion Coulomb energy $q^2/(\epsilon a_\perp)$: $\tilde{U} = U\epsilon a_\perp/q^2 = 4U\epsilon/(\pi a_\perp q\sigma_s)$. In this rescaled form, the result would explicitly depend on neither ion valency nor the surface charge density. If we also suppose that the ions form a perfect crystal so that each ion has exactly the same environment, one summation over all ions can be performed right away. Thus, we get for the energy per ion

$$\frac{\tilde{U}_1}{N} = a_\perp \sum_{j=2}^N \frac{1}{|\mathbf{r}_j - \mathbf{r}_1|} - \frac{8R}{a_\perp} \quad (2)$$

For two such plates, in case they are parallel to each other and have identical ion configurations, the total energy will contain the self-energy, $2U_1$, plus the interaction terms: ions – opposite plate and plate–plate. The ion–plate and plate–plate energies in the case of charge neutrality will compensate each other as the sum of distances from each ion of charge q to the two plates is always $h + 2R$, which is exactly equal to the distance between the corresponding surface element of the same net charge and the opposite plate. Then the only interesting contribution comes from the summation over the ions

$$\begin{aligned} \frac{\tilde{U}_{12}(h)}{N} &= a_\perp \sum_{j=2}^N \frac{1}{|\mathbf{r}_j - \mathbf{r}_1|} \\ &+ a_\perp \sum_{k=1}^N \frac{1}{\sqrt{(\mathbf{r}_k - (\mathbf{r}_1 + \mathbf{a}))^2 + (h + 2R)^2}} \end{aligned} \quad (3)$$

where h the distance between the ion-containing planes, thus giving the distance between the plates $h + 2R$, and \mathbf{a} the displacement vector of the lattice on one plate with respect to the other one. The indices j and k now mean a summation over the ions on different plates. As the interlayer interaction leads to structural transformation within the layer, these two terms remain interconnected and should always be considered simultaneously. For infinite plates, the total Coulomb energy has to be calculated numerically. We modeled a piece of 2D crystal of size 40×40 to 80×80 ions with lateral periodic boundary conditions, and calculated the energies with relative uncertainty of 10^{-6} . The plates were supposed to be homogeneously charged. An MMM2D summation scheme [29] and an MD simulation package ESPResSo v. 1.9 were used [30].

We first consider the relative energies of the preformed lattices. Figure 2 shows the potential energy of interaction between the two layers as a function of the gap width h for the three setups. The total energy, $U = 2U_1 + U_{12}$, in all of them is strongly negative and decreases in absolute value with the gap width. The limiting value at $h \rightarrow \infty$ on each curve corresponds to twice the energy of a single Wigner crystal U_1 . To calculate the true ground state energy we

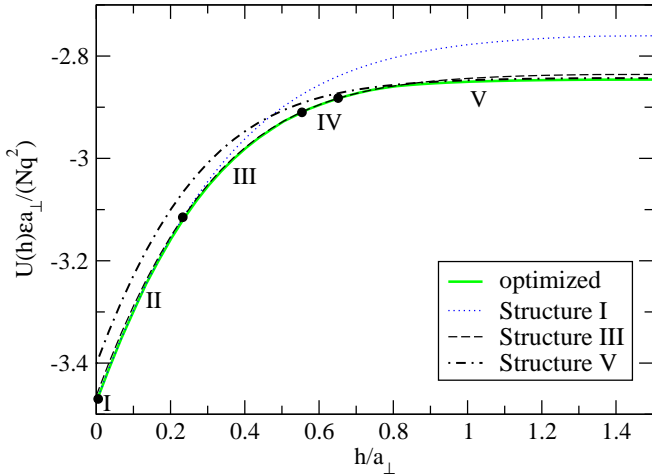


Fig. 2: Rescaled potential energy per ion of two parallel Wigner crystals on oppositely charged plates as a function of normalized distance h/a_{\perp} between the crystals for the three different counterion arrangements. The optimized structure is obtained by the energy minimization using a Brownian dynamics simulation at zero temperature. The transition points as reported in Ref. [14] are marked by filled circles. The regions of stability of various crystalline structures are delimited by the circles and marked next to the optimized energy curve.

perform molecular dynamics simulation of two ionic layers with the ions constrained to their corresponding planes but allowed to move within the plane. For each interlayer distance we start simulation from each of the three preformed lattices and then record the minimal energy. We see that the minimal energy from the free configuration coincides with energy of the favorable arrangement in the appropriate range of distances and gets lower in two intermediate regions close to the transition points I \rightarrow III and III \rightarrow V (Fig. 2). In these regions, one should expect an appearance of the staggered rectangular lattice and the staggered rhombic one, respectively. At $h = 0$ we obtain the rescaled energy per ion $\tilde{U}_{12} = -3.47502$, which is close to value -3.47493 reported in Ref. [14] (the scaling factor in our work differs from Ref. [14] by $\sqrt{\pi}$). The single hexagonal lattice is stable in a very small region close to $h/a_{\perp} = 0$. The location of the further transition points can be estimated from comparing the energies of the corresponding phases. The intersection point of the curves I and III in Fig. 2 corresponds to a transition into staggered square phase. The energy of the optimized structure becomes lower than that of the phase III at $h/a_{\perp} \approx 0.55$, which indicates a transition into phase IV. The structure V prevails at $h/a_{\perp} \geq 0.77$. We note that the transition in our work is observed at a higher h/a_{\perp} than it was reported in [14,18]. The interaction energy of the two layers is shown in Fig. 3a. The energy curve is smooth between the transition points. The force curve shows a jump at $h/a_{\perp} \approx 0.77$, which is expected due to discontinuous character of the transition between

phases IV and V [14]. The initial decay of the interaction energy is close to linear, while the asymptotic behaviour at $h/a_{\perp} > 1$ is clearly exponential. The observed behaviour is close to the asymptotic decay expected at large distances $U_{12}(h) \propto \exp(-h/(a_{\perp}/2\pi))$ [12,14] (see Fig. 2).

We now look at the interaction between crystals formed by Coulombic dimers for two different lateral ion sizes $L = 0.5R = 0.17a_{\perp}$ and $L = R = 0.34a_{\perp}$. As an additional degree of freedom is involved, we expect a richer phase behaviour in this case. In the limit $L = 0$ the behaviour of the system with point-like ions is recovered. Figure 3b presents the interaction energies as a function of the gap width. Simulation snapshots for three different values of $h/a_{\perp} = 0.1, 0.33, 0.5, 0.75$ and 1.2 , which correspond to different crystalline structures, are presented in Figure 4. We see that at small and large relative distances the dimers in the two layers tend to be aligned while at the intermediate separations the dimers in each layer tend to orient perpendicular to their nearest neighbors in the 2D projection of the lattice (either same plane neighbors or the neighbors in the opposite plane).

A variation of the dimer length affects only the ion-ion part of the total energy of the bilayer. A system with longer dimers has a higher self-energy of each layer while the corresponding interlayer part depresses the interaction. We see from Fig. 3b that the interaction between the layers indeed becomes weaker on increasing the dimer length. Roughly, the characteristic length a_{\perp} decreases by $L/2$ as compared to the point charges. Then, the interaction energy would decay as $U(h) \propto \exp(2\pi h/(a_{\perp} + L/2))$. A fit to the calculated interaction energies reveals the decay length change from $0.19a_{\perp}$ for the point-like ions to $0.15a_{\perp}$ for the system with $L = 1$ (or $0.34a_{\perp}$). Ultimately, at $L = a_{\perp}$ at small separations one should recover the bilayer with $a'_{\perp} = a_{\perp}/\sqrt{2}$.

In simulations with short dimers with $L = 0.17a_{\perp}$ at various gap thicknesses we observe: (i) $0 < h/a_{\perp} < 0.27$ a staggered parallelogrammatic lattice, parallel orientation of neighboring dimers, soft; (ii) $0.27 < h/a_{\perp} < 0.8$ staggered square lattice, perpendicular dimer orientation, rigid; (iii) $0.8 < h/a_{\perp}$ staggered rhombic lattice, parallel dimer orientation, rigid. At $L = 0.34a_{\perp}$, we have the following sequence of structures: (i) $0 < h/a_{\perp} < 0.17$ a staggered rectangular lattice, parallel orientation of neighboring dimers, rigid, the longer lattice constant a_2 is roughly $a_1 + L$ (Fig. 4a); (ii) $0.17 < h/a_{\perp} < 0.40$ we observe domains of rhombic lattice, rotated with respect to the neighbouring domains (Fig. 4b); (iii) $0.40 < h/a_{\perp} < 0.67$ staggered square lattice, perpendicular dimer orientation, rigid (Fig. 4c); (iv) $0.67 < h/a_{\perp} < 0.91$ staggered parallelogrammatic lattice, parallel dimer orientation, rigid (Fig. 4d); (v) $0.91 < h/a_{\perp}$ staggered triangular (a honeycomb-like) lattice, parallel, rigid (Fig. 4e). We note that in contrast with some phases of point ions (the "soft" rectangular (II) and rhombic (IV) phases), the observed lattices in the system with long dimers ($L = 0.34a_{\perp}$) are rigid, i.e. the aspect ratio of the primitive cell stays constant within

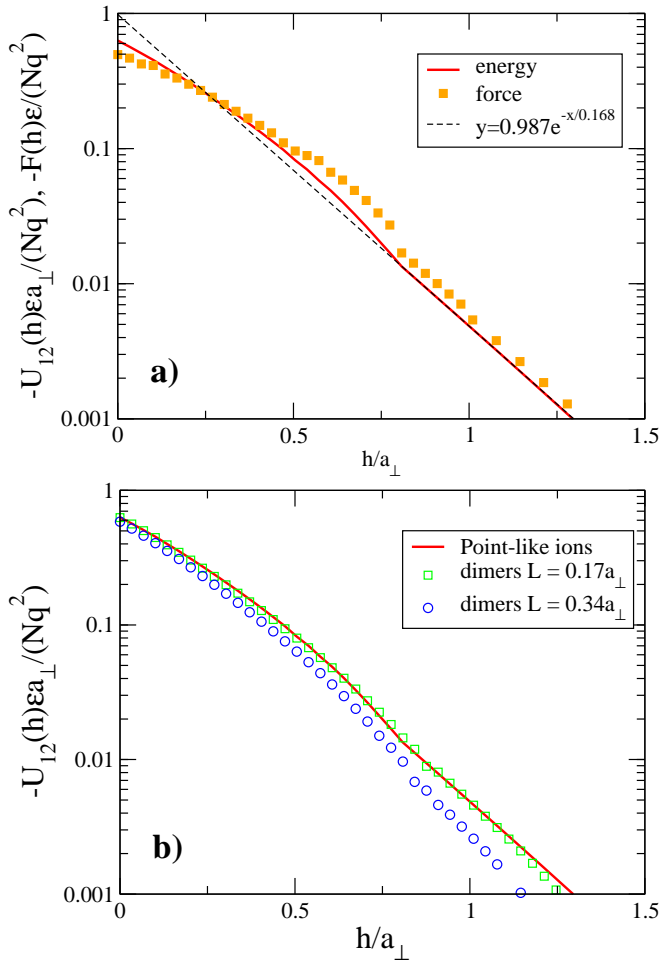


Fig. 3: a) Absolute value of rescaled attraction energy and force between two charged plates with crystalline arrangement of point-like ions. The dashed line shows the predicted asymptotic behaviour at large h/a_{\perp} [14]. b) The rescaled interaction energy between two parallel Wigner crystals formed by charged dimers of the indicated length in comparison with that for point-like ions. The dimer charge as well as the number density are matching those for the system with point-like ions.

the region of stability of the corresponding lattice.

The most interesting observation for the dimeric systems is related to the ability of dimers to adjust the orientation to minimize the electrostatic energy. The effect is strongest for the square lattices where we find perpendicular orientation of the neighboring dimers. A similar phenomenon of altering orientational ordering was discussed recently for a one-dimensional stack of rod-like ions [31]. In contrast to our observation for 2D layers, the ground state in a staggered 1D system is represented by perpendicular orientation of the neighboring ions, which then changes to a twisted chiral phase on increasing density. In our system, the reorientation of the ions happens suddenly on varying the separation distance between the surfaces, which might find an application in nano-structuring. This structural transformation can be best characterized by the

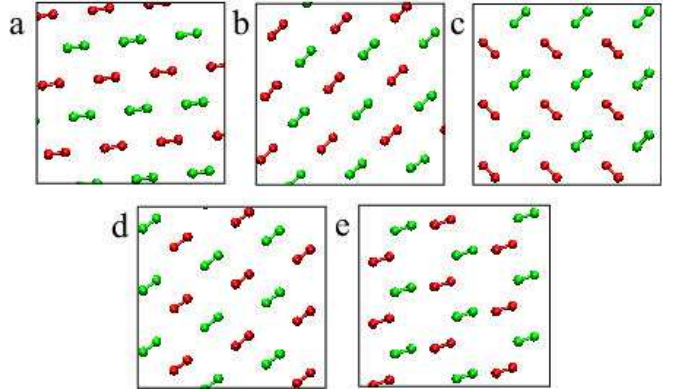


Fig. 4: Snapshots from simulations of dimeric bilayers with dimer length $L = 0.34a_{\perp}$ at different gap widths: $h/a_{\perp} = 0.1$ (a), 0.33 (b), 0.5 (c), 0.75 (d), 1.2 (e). The different colors correspond to ions located at different planes.

scalar order parameter $S = \frac{1}{2}\langle 3 \cos^2 \theta - 1 \rangle$ (the second moment of the orientational distribution function), where θ is the angle between the molecule orientation and the director, and average over all dimers is taken. This value is plotted in Fig. 5. One can see that the phases at short and long interlayer distances have $S = 1$, which corresponds to ideally aligned dimers (Fig. 4a,d,e). Further on, the S values of 0.25 correspond to a coexistence of two preferred dimer orientations (Fig. 4c), which are perpendicular to each other. The arrangements with two preferred orientations are observed in the region of stability of the square lattice. From the plot shown in Fig. 5, we see that the onset of the perpendicular dimer orientation as well as the return into the aligned state happens in the system with longer dimers at smaller distances.

Finally, we note that the presented sequence of orientational transitions exists also at finite temperatures. A simulation performed for $L/a_{\perp} = 0.34$ at $\Xi = 50000$ and $\Xi = 10000$ still showed three regions with high, then low, and again high order parameter on increasing the interlayer distance, although the short-distance and the long-distance phases become less aligned due to thermal fluctuations. The observed order parameter was $S \approx 0.9$ at small interlayer separations, and $S \approx 0.8$ ($\Xi = 50000$) and $S \approx 0.4$ ($\Xi = 10000$) at large separations (Fig. 5, triangles), while the values for the perpendicular dimer orientations, $S \approx 0.25$, did not change with temperature. One can expect that the temperature region of stability of the square lattice with the perpendicular dimer orientation is larger than that for the aligned phases, which follows from the increasing stability of the square lattice itself in the system with point ions [16]. We also note that the bilayer system is stable with respect to normal fluctuations, which are suppressed in our setup by the repulsion between the mobile ions that confines the ions to thin layers at the walls.

We calculated the ground state interaction energy of two

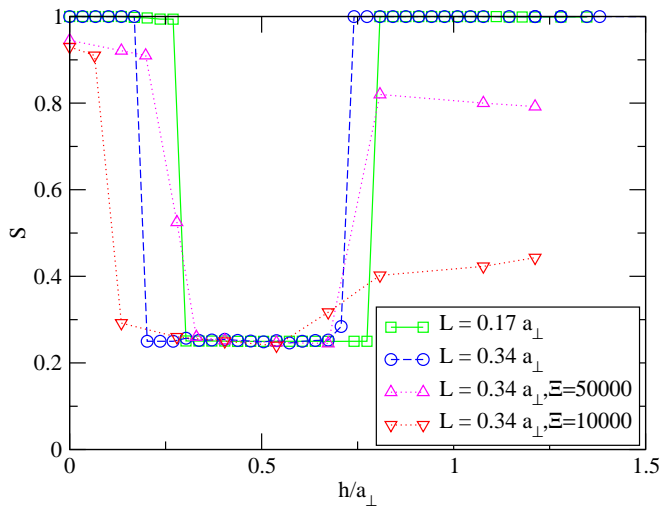


Fig. 5: Orientational order parameter for dimeric Wigner bilayers with two different dimer sizes. The value $S = 1$ corresponds to perfectly aligned dimers, $S = 0.25$ to a coexistence of two perpendicular dimer orientations. The lines are guide to the eye.

planar ionic double layers represented by Wigner crystals of point-like charges or charged dimers, where the latter model mimics the situation of screening the interaction between charged surfaces with polyelectrolytes or non-spherical molecules. The crystalline structure observed with point-like charges agrees with that reported in the earlier literature, while novel structures with unusual orientational ordering were observed in the system with elongated ions. In all cases we found exponential asymptotic decay of the correlation attraction at interlayer distances larger than the characteristic lateral separation between the counterions. We found that the elongated ions produce in general weaker correlation attraction than the point-like or spherical ions of the same charge.

We are grateful to F. M. Peeters for introducing us to his works on bilayer Wigner crystals and for his comments on the manuscript. The work was partly supported by a program “Material Science of Complex Interfaces” of Elitenetzwerk Bayern.

REFERENCES

- [1] GULDBRAND L., JÖNSSON B., WENNERSTRÖM H. and LINSE P., *J. Chem. Phys.*, **80** (1984) 2221.
- [2] LINSE P., LOBASKIN V., *Phys. Rev. Lett.*, **83** (1999) 4208.
- [3] LOBASKIN V., LYUBARTSEV A., LINSE P., *Phys. Rev. E*, **63** (2001) 020401.
- [4] KÉKICHEFF P., MARČELJA S., SENDEN T. J. and SHUBIN V. E., *J. Chem. Phys.*, **99** (1993) 6098.
- [5] LI L., HARNAU L., ROSENFELDT S. and BALLAUF M., *Phys. Rev. E*, **72** (2005) 051504.
- [6] DUBOIS M., ZEMB T., FULLER N., RAND R. P. and PARSEGIAN V. A., *J. Chem. Phys.*, **108** (1998) 7855.
- [7] KHAN A., JÖNSSON B. and WENNERSTRÖM H., *J. Phys. Chem.*, **89** (1985) 5180.
- [8] LEVIN Y., *Rep. Prog. Phys.*, **65** (2002) 1577.
- [9] GROSBERG A. YU., NGUYEN T. T., SHKLOVSKII B. I., *Rev. Mod. Phys.*, **74** (2002) 329.
- [10] BOROUDJERDI H., KIM Y.-W., NAJI A., NETZ R. R., SCHLAGBERGER X., SERR A., *Phys. Rep.*, **416** (2005) 129.
- [11] NAJI A., JUNGBLUT S., MOREIRA A. G., and NETZ R. R., *Physica A*, **352** (2005) 131.
- [12] ROUZINA I. and BLOOMFIELD V. A., *J. Phys. Chem.*, **100** (1996) 9977.
- [13] SHKLOVSKII B. I., *Phys. Rev. Lett.*, **82** (1999) 3268.
- [14] GOLDONI G. and PEETERS F. M., *Phys. Rev. B*, **53** (1996) 4591.
- [15] FALCO V. I., *Phys. Rev. B*, **49** (1994) 7774.
- [16] SCHWEIGERT I. V., SCHWEIGERT V. A., and PEETERS F. M., *Phys. Rev. B*, **60** (1999) 14665.
- [17] SCHWEIGERT I. V., SCHWEIGERT V. A., and PEETERS F. M., *Phys. Rev. Lett.*, **82** (1999) 5293.
- [18] WEISS J. J., LEVESQUE D., and JORGE S., *Phys. Rev. E*, **63** (2001) 045308.
- [19] SUEN Y. W., ENGEL L. W., SANTOS M. B., SHAYEGAN M., and TSUI D. C., *Phys. Rev. Lett.*, **68** (1992) 1379.
- [20] STRANDBURG K. J., *Rev. Mod. Phys.*, **60** (1988) 161.
- [21] LAU A. W. C., LEVINE D., and PINCUS P., *Phys. Rev. Lett.*, **84** (2000) 4116.
- [22] LAU A. W. C., PINCUS P., LEVINE D., and FERTIG H. A., *Phys. Rev. E*, **63** (2001) 051604.
- [23] TRAVESSET A. and VAKNIN D., *Europhys. Lett.*, **74** (2006) 181.
- [24] BOUYER F., ROBBEN A., YU W. L. and BORKOVEC M., *Langmuir*, **17** (2001) 5225.
- [25] LIN W., GALETTO P., BORKOVEC M., *Langmuir*, **20** (2004) 7465.
- [26] TURESSON M., FORSMAN J., ÅKESSON T., *Langmuir*, **22** (2006) 5734.
- [27] SALDITT T., KOLTOVER I., RÄDLER J. O., SAFINYA S. R., *Phys. Rev. Lett.*, **79** (1997) 2582.
- [28] O’HERN C. S., LUBENSKY T. C., *Phys. Rev. Lett.*, **80** (1998) 4345.
- [29] ARNOLD A. and HOLM C., *Comp. Phys. Communications*, **148** (2002) 327
- [30] LIMBACH H.-J., ARNOLD A., MANN B. A., and C. HOLM, *Comp. Phys. Communications*, **174** (2006) 704
- [31] FAZLI H., GOLESTANIAN R., and KOLAHCHI M. R., *Phys. Rev. E*, **72** (2005) 011805.